
Satellite Products and Services Review Board

Algorithm Theoretical Basis Document For NOAA NDE VIIRS Active Fire

Compiled by the
SPSRB Common Standards Working Group



Version 2.6
June, 2016

TITLE: VIIRS ACTIVE FIRE ALGORITHM THEORETICAL BASIS DOCUMENT

AUTHORS:

Louis Giglio (University of Maryland)

Wilfrid Schroeder (University of Maryland)

Ivan Csiszar (NOAA/NESDIS Center for Satellite Applications and Research)

Marina Tsidulko (I.M. Systems Group, Inc.)

Remarks: This document shares algorithm descriptive material with the corresponding NASA-sponsored VIIRS Active Fire algorithm theoretical basis document.

**DOCUMENT HISTORY
 DOCUMENT REVISION LOG**

The Document Revision Log identifies the series of revisions to this document since the baseline release. Please refer to the above page for version number information.

DOCUMENT TITLE: Algorithm Theoretical Basis Document Template			
DOCUMENT CHANGE HISTORY			
Revision No.	Date	Revision Originator Project Group	CCR Approval # and Date
1.0			

TABLE OF CONTENTS

	<u>Page</u>
LIST OF TABLES AND FIGURES.....	6
1. INTRODUCTION.....	7
1.1. Product Overview.....	7
1.1.1. Product Description	7
1.1.2. Product Requirements.....	9
1.2. Satellite Instrument Description.....	9
2. ALGORITHM DESCRIPTION	9
2.1. Processing Outline.....	10
2.2. Algorithm Input	10
2.3. Theoretical Description	11
2.3.1. Physical Description	11
2.3.2. Mathematical Description	12
2.4. Algorithm Output	15
2.5. Performance Estimates.....	16
2.5.1. Test Data Description.....	16
2.5.2. Sensor Effects	17
2.5.3. Retrieval Errors.....	20
2.5.4. Numerical Computation Considerations.....	20
2.5.5. Programming and Procedural Considerations	20
2.5.6. Quality Assessment and Diagnostics	21
2.5.7. Exception Handling.....	22
2.6. Validation.....	22
3. ASSUMPTIONS AND LIMITATIONS.....	24
3.1. Performance Assumptions	24
3.2. Potential Improvements	24
4. REFERENCES.....	25

LIST OF TABLES AND FIGURES

Table 2-1: List of input data sets used in the VIIRS AF algorithm. All input data sets have a nominal resolution of 750 m..... 11

Table 2-2: VIIRS AF science data sets. Variable *n* indicates the number of 48-scan blocks found in a single granule (*n*=1 for NDE granule) (see Section 1.1.1). 16

Figure 1-1: VIIRS AF fire mask (native swath projection) over an area in Northern Canada derived from a VIIRS granule acquired approximately at 20:06 UTC on 29 May 2015. 8

Figure 2-1: VIIRS AF algorithm processing flow. Input data are gathered (SDR) and pre-processed (granulation of land/water mask), and ingested into the fire detection module for scan *i* along with scan *i*-1 and *i*+1 used in the contextual analyses. Finally FRP is calculated for each fire pixel detected..... 10

Figure 2-2: Spectral radiance for average land, flaming, and smoldering fire temperatures, and the spectral response functions of all six VIIRS channels used by the AF algorithm. 12

Figure 2-3: Percentage of M15 aggregated pixels resulting from the mixing of saturated and un-saturated native pixels. Results were generated using simulated VIIRS data based on actual Advanced Spaceborne Thermal Emission and Reflection Radiometer (ASTER) 30-m resolution fire-affected pixels. 18

Figure 2-4: Spectral response functions for VIIRS I4 and M13, and MODIS B21/22 mid-infrared channels, and the corresponding atmospheric transmittance calculated using MODTRAN assuming U.S. standard atmospheric conditions (top panel). Bottom panel shows the corresponding net atmospheric absorption as a function of scan angle..... 19

Figure 2-5: S-NPP/VIIRS AF and Aqua/MODIS MYD14 fire detection data produced for the King fire/California on 14-19 September 2014. 22

Figure 2-6: Validation of VIIRS AF active fire pixels (marked in thick dashed lines) using airborne reference fire data (background color image, active fires in yellow-red shades) during the Prescribed Fire Combustion and Atmospheric Dynamics Research (RxCADRE) experiment at Eglin Air Force Base/FL, 10 November 2012. 23

1. INTRODUCTION

This document presents the scientific background, design and anticipated performance of the Active Fire (AF) algorithm for the Joint Polar Satellite System (JPSS). The AF algorithm produces two main outputs from the Visible Infrared Imaging Radiometer Suite (VIIRS) 750 m multi-spectral data, namely: (i) an image classification product (fire mask) including thematic classes such as fire/no-fire, clouds, water and clear-land pixels; and (ii) sub-pixel characterization of the instantaneous power emitted by detected fires (fire radiative power [FRP] retrievals).

The VIIRS AF algorithm described here fulfills the requirements identified in the JPSS Active Fire Environmental Data Record (EDR) specification (JPSS L1RDS.5.5.1), while addressing other user-driven requirements meant to facilitate product usage and assimilation onto ongoing fire research and applications (e.g., science data formats and nomenclature). Furthermore, those requirements provide continuity to the Moderate Resolution Imaging Spectroradiometer (MODIS) and the Advanced Very High Resolution Radiometer (AVHRR) active fire data records. The VIIRS AF algorithm builds on the 1 km MODIS *Fire and Thermal Anomalies* (MOD14/MYD14) Collection 6 product, incorporating code updates and methodological advances derived from several years of algorithm development and validation [Giglio et al., 2016].

1.1. Product Overview

1.1.1. Product Description

The VIIRS AF product is a Level 2 data set retaining the original swath projection and geolocation information of the Level 1 input data used. A single file (or granule) comprises an orbit segment spanning multiple scans, with each individual cross-track scan describing 16 rows of pixels (Y axis), one row for each detector. Each scan row contains a total of 3200 samples (X axis) consisting of 750 m nominal resolution pixels. The number of scans stored in a single file may vary depending on the characteristics of the data processing system, whereas multiples of 48 are used. As a result, the minimum array size of the fire mask included in the VIIRS AF product will have $n=1 \times 48$ scans, or 3200×768 elements corresponding to an ≈ 86 second orbit segment. The Suomi NPP Data Exploitation (NDE) system operating the AF algorithm at NOAA/NESDIS, by default, processes each ≈ 86 second granule separately. The VIIRS AF algorithm is applied to every pixel in the input day and nighttime data files, extending the detection of fires over ocean waters to allow

mapping of offshore gas flaring in response to users' requests. Coastlines and inland water bodies are normally skipped during processing in order to avoid potential false alarms. Those areas are identified and masked using ancillary land/water classification data (see Section 2.2).

The image classification product (fire mask) is the primary science data set consisting of a two dimensional array with same size as the input VIIRS 750 m data used by the fire algorithm. The VIIRS AF fire mask contains nine different pixel classes; three of those classes are used to flag fire-affected pixels along with their detection confidence (see Section 2.4). FRP retrievals and other supporting data such as fire pixel image element [x] and [y], and latitude/longitude are stored in vector format, each containing *N* records describing the number of fire pixels detected (See Table 2-4).

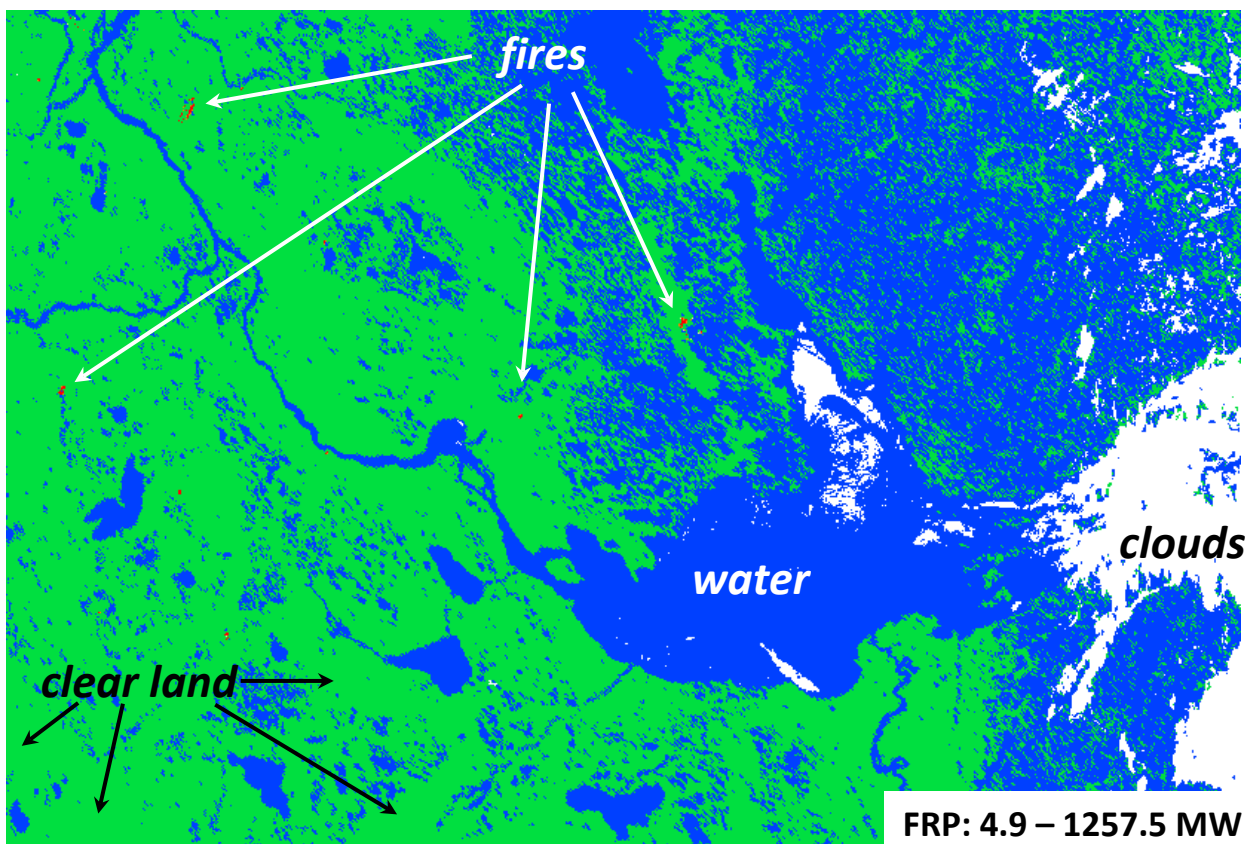


Figure 1-1: VIIRS AF fire mask (native swath projection) over an area in Northern Canada derived from a VIIRS granule acquired approximately at 20:06 UTC on 29 May 2015.

1.1.2. Product Requirements

The requirements for the VIIRS active fire product are described in the JPSS Level 1 Requirements Supplement. (The current version is available at http://www.jpss.noaa.gov/technical_documents.html .)

1.2. Satellite Instrument Description

The AF algorithm uses data from the VIIRS instrument on the Suomi National Polar-orbiting Partnership (S-NPP) platform and on future satellites of the Joint Polar Satellite System (JPSS). S-NPP was launched on October 28, 2011. It is in a sun synchronous orbit with a 1:30pm ascending-node orbit at an altitude of 829 km.

The VIIRS instrument is a whiskbroom scanning radiometer with a swath width of 3060 km, providing full daily coverage both in the day and night side of the Earth. It has 22 spectral bands covering the spectrum between 0.412 μm and 12.01 μm , including 16 moderate resolution bands (M-bands) with a spatial resolution of 750 m at nadir, 5 imaging resolution bands (I-bands) – with a spatial resolution of 375 m at nadir, and one panchromatic DNB with a 750 m spatial resolution throughout the scan. Further details can be found in the VIIRS Sensor Data Record (SDR) User's Guide (NOAA Technical Report NESDIS 142A).

2. ALGORITHM DESCRIPTION

The AF algorithm provides active fire detection and characterization information for each VIIRS granule, resulting in daily global coverage for daytime and nighttime observations. Different sets of detection criteria are used during day and night observations; night pixels are defined as those having a solar zenith angle greater than 85° . The detection criteria are based on multi-spectral tests using primarily the mid-infrared (3.973-4.128 μm) channel M13 and thermal-infrared (10.263-11.263 μm) channel M15 brightness temperature of the candidate fire pixel, and the brightness temperature difference between that pixel and its background (neighboring pixels). Those primary detection tests are complemented by other multi-spectral tests based on the reflective channels (M05, M07, and M11 – daytime detection only) and the long-wave thermal-infrared channel (M16) in order to screen for other radiometrically bright pixels (e.g., clouds and sandy soil) that can lead to false alarms. The algorithm uses a hybrid approach to detect fires based on fixed thresholds and dynamically adjusted contextual tests. The latter utilize sampling windows of variable sizes to assess the areas surrounding candidate fire pixels. The use of adaptive detection tests allows for improved algorithm response to sub-pixel fire activity across a wide range of observation conditions.

2.1. Processing Outline

The VIIRS AF is a self-contained algorithm with no dependencies on other Level 2 products. It reads input SDR from up to six VIIRS 750 m channels, plus the companion terrain-corrected geolocation file and the land/water mask (see Section 2.2). The latter is derived from VIIRS Global Surface Type data, which is converted into swath granules to match the input SDR file format. The input (read) module feeds three full scans (16 lines each) at a time to the fire detection module in order to (i) meet requirements of contextual tests (i.e., sampling of background pixels using a dynamic window, expandable to a maximum of 21×21 pixels), and (ii) minimize memory usage. FRP are calculated for all fire pixels detected.

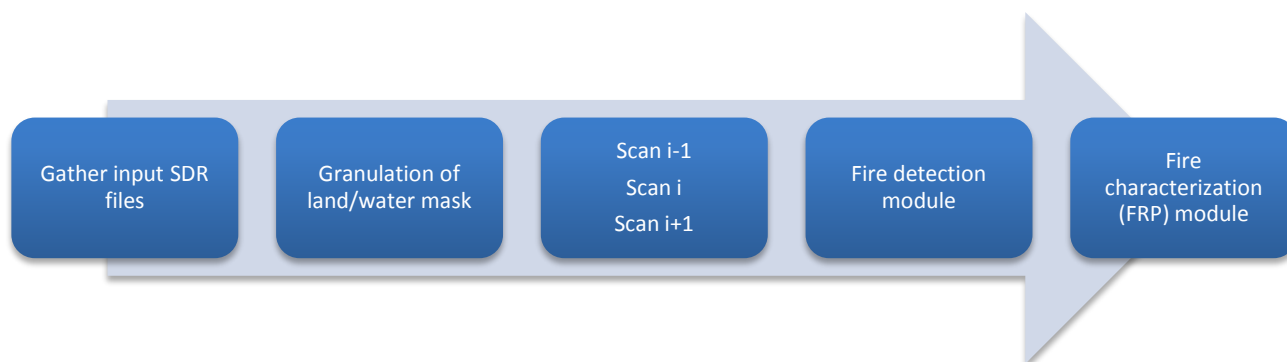


Figure 2-1: VIIRS AF algorithm processing flow. Input data are gathered (SDR) and pre-processed (granulation of land/water mask), and ingested into the fire detection module for scan i along with scan $i-1$ and $i+1$ used in the contextual analyses. Finally FRP is calculated for each fire pixel detected.

2.2. Algorithm Input

The input data sets used by the VIIRS AF algorithm are listed in Table 2-1. All input data derived from VIIRS SDR Level 1 files are used in their original swath projection format. All radiance, reflectance, and brightness temperature data correspond to the calibrated top-of-atmosphere (at-sensor) values. The complementary SDR quality flag (QF1) information is used to help identify pixels showing non-nominal data quality as a result of poor-calibration, pixel saturation and other data artifacts. The QF1 data are used judiciously in order to identify and avoid SDR data artifacts, thereby preventing spurious detections in the resulting AF product. A single ancillary data set derived from gridded Global Surface Type data is used in support of land/water classification. The Global Surface Type data is an annual product with global coverage. A granulation process is implemented to that data set in order to create data arrays of identical dimensions and projection type as the input SDR files. All algorithm inputs describe the nominal VIIRS 750 m aggregated data.

Table 2-1: List of input data sets used in the VIIRS AF algorithm. All input data sets have a nominal resolution of 750 m.

Input	Data Sets	Primary Use
M05 channel SDR (0.662-0.682 μm)	<ul style="list-style-type: none"> At-sensor reflectance (unitless) Quality Flag 1 (QF1) (unitless) 	Cloud screening, and sun glint and coastal false alarm rejection
M07 channel SDR (0.846-0.885 μm)	<ul style="list-style-type: none"> At-sensor reflectance (unitless) Quality Flag 1 (QF1) (unitless) 	Cloud screening, and sun glint and coastal false alarm rejection
M11 channel SDR (2.225-2.275 μm)	<ul style="list-style-type: none"> At-sensor reflectance (unitless) Quality Flag 1 (QF1) (unitless) 	Sun glint and coastal false alarm rejection
M13 channel SDR (3.973-4.128 μm)	<ul style="list-style-type: none"> At-sensor radiance ($\text{W}\cdot\text{m}^{-2}\cdot\text{sr}^{-1}\cdot\mu\text{m}^{-1}$) and brightness temperature (K) Quality Flag 1 (QF1) (unitless) 	Fire detection and fire radiative power retrieval
M15 channel SDR (10.263-11.263 μm)	<ul style="list-style-type: none"> At-sensor brightness temperature (K) Quality Flag 1 (QF1) (unitless) 	Fire detection
M16 channel SDR (11.538-12.488 μm)	<ul style="list-style-type: none"> At-sensor brightness temperature (K) Quality Flag 1 (QF1) (unitless) 	Cloud screening
Terrain-corrected geolocation	<ul style="list-style-type: none"> Latitude & Longitude (decimal degrees) Satellite zenith & azimuth (decimal degrees) Solar zenith & azimuth (decimal degrees) 	Fire pixel geolocation
MODIS 1 km land/water mask	<ul style="list-style-type: none"> Land water mask (unitless) 	Land & water classification

2.3. Theoretical Description

2.3.1. Physical Description

Actively burning fires often show a wide range of temperatures spanning several hundred Kelvin in association with flaming and smoldering phases of combustion. Typically, cooler smoldering fires show temperatures between 450 and 850 K, whereas higher temperatures ranging from 800 K to upwards of 1200 K prevail during the more intense flaming phase [Lobert and Warnatz, 1993]. Fuel type and moisture, and ambient conditions (air temperature, wind, and relative humidity) are key factors regulating combustion. When moderate spatial resolution sensors are considered, mid-infrared (4 μm) spectral channels are the most responsive to actively burning fires capturing most of the radiometric signal from smoldering and flaming phases of combustion during both day and nighttime parts of the orbit. Figure 2-2 shows the Planck function curves applied to targets of distinct temperatures, and the spectral response functions of all six VIIRS channels used in the AF algorithm. Based on its spectral and radiometric characteristics, which includes a dual-gain configuration for extended dynamic range (650 K saturation temperature), channel M13 is the primary driver of the VIIRS AF algorithm. The peak in emitted fire radiant energy on channel M13 makes that channel responsive to small sub-pixel fires occurring over a cool

(≈ 300 K) background. Consequently, intense active fires (>1000 K) occupying fractional pixel areas as small as 10^{-4} may be detected.

In addition to facilitating the detection of sub-pixel active fires, the rate of radiative energy released by fires (FRP) observed in the $4 \mu\text{m}$ region is found to be directly related to the biomass consumed per unit time [Kaufman *et al.*, 1998; Wooster *et al.*, 2003]. Starting with the launch of the Terra/MODIS sensor in 1999, which for the first time provided unsaturated mid-infrared observations over a wide range of fire conditions, FRP retrievals were introduced as a complement to the standard fire detection product [Justice *et al.*, 2002]. The VIIRS AF algorithm builds on the MODIS heritage also incorporating FRP retrievals for all fire pixels detected.

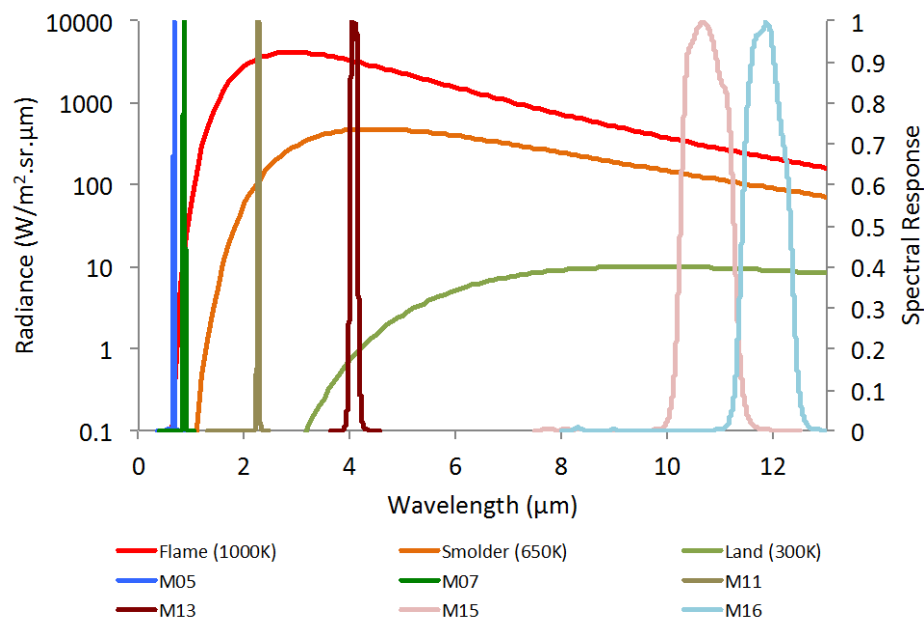


Figure 2-2: Spectral radiance for average land, flaming, and smoldering fire temperatures, and the spectral response functions of all six VIIRS channels used by the AF algorithm.

2.3.2. Mathematical Description

The VIIRS AF algorithm is composed of a series of fixed-threshold and contextual tests that, when applied to a candidate pixel, will indicate the presence of sub-pixel fire activity provided those tests are satisfied. The processing scheme can be divided into three main parts, namely: (i) detection of unambiguous fire pixels, (ii) identification of candidate fire pixels, and (iii) detection of fire pixels selected in step (ii).

The detection of unambiguous fire pixels is accomplished with the following fixed threshold tests:

Test 1: Daytime: $T_{13} > 360$ K; Nighttime: $T_{13} > 320$ K

Where T_{13} is the brightness temperature on channel M13.

Before other candidate fire pixels can be selected, an internal cloud masking procedure is applied to all image pixels using the following set of conditions:

$(\rho_5 + \rho_7) > 1.2$ (daytime only)
or
 $(\rho_5 + \rho_7) > 0.7$ and $T_{16} < 285$ K (daytime only)
or
 $T_{16} < 265$ K
or
water pixel AND $\rho_7 > 0.25$ AND $T_{16} < 300$ K

Where ρ_i is the reflectance on VIIRS M channel i , and T_{16} is the brightness temperature on channel M16. Following the screening of cloud pixels, candidate fire pixels are selected based on the following criteria:

Daytime: $T_{13} > T_{13}^*$ and $\Delta T_{13-15} > \Delta T_{13-15}^*$ AND $\rho_7 < 0.35$

Nighttime: $T_{13} > T_{13}^*$ and $\Delta T_{13-15} > \Delta T_{13-15}^*$

Here ΔT_{13-15} represents the brightness temperature difference between channel M13 and M15. The T_{13}^* and ΔT_{13-15}^* thresholds are the mean background values calculated using a large sampling window centered in the candidate pixel after exclusion of clouds, water and other candidate fire pixels. Next, the following sequence of commands is performed:

- I. Conduct search in geometric neighborhood of potential fire pixel, ranging from 3x3 pixel box (centered at the candidate fire pixel) to 21x21 pixels.
- II. For each valid clear land pixel in the geometric neighborhood:
 - a. Determine if the pixel is a background fire pixel:
Daytime: $T_{13} > 325$ K and $\Delta T_{13-15} > 20$ K
Nighttime: $T_{13} > 310$ K and $\Delta T_{13-15} > 10$ K
 - b. Other clear land pixels are flagged as valid background pixels
- III. Accumulate valid background pixel data for statistics on T_{13} , T_{15} , and ΔT_{13-15}
 - a. Compute:
 Nt = number of non-fill pixels in neighborhood search
 Nb = number of valid background pixels in neighborhood search

$Fb = Nb/Nt$; fraction valid background pixels

- IV. If [$Fb \geq 25\%$ AND $Nb \geq 8$] then exit neighborhood search loop; otherwise, search over next larger region
 - a. If the neighborhood search is unsuccessful, flag pixel as unknown and continue with next pixel for fire test; else proceed to next step
- V. Compute aggregate statistics over selected search region:
 - Means for valid background pixels (T_{13B} , T_{15B} , and $\Delta T_{13B-15B}$)
 - Mean absolute deviations for valid background pixels (δT_{13B} , δT_{15B} , and $\delta \Delta T_{13B-15B}$)
 - Mean absolute deviations for background fires (T'_{13B} and $\delta T'_{13B}$)

Once neighboring statistics are calculated, the contextual fire tests are applied using:

Test 2: $\Delta T_{13-15} > \Delta T_B + 3.5 \delta \Delta T_B$

Test 3: $\Delta T_{13-15} > \Delta T_B + 6 K$

Test 4: $T_{13} > T_{13B} + 3 \delta T_{13B}$

Test 5: $T_{15} > T_{15B} + \delta T_{15} - 4 K$ (daytime only)

Test 6: $\delta' T_{13B} > 5 K$ (daytime only)

Assign fire class if the following tests are satisfied:

Daytime: Test 1 or [Test 2 and Test 3 and Test 4 {Test 4 or Test 5}]

Nighttime: Test 1 or [Test 2 and Test 3 and Test 4]

Finally, complementary tests are applied in order to exclude potential false alarms associated with sun glint, forest clearings, coastal areas and pixels in false-alarm prone background. Fire pixels (excluding unambiguous fires) satisfying any of the conditions below are rejected:

- I. Sun glint:

Define Θ_g as $\arccos(\cos\Theta_v \cos\Theta_s - \sin\Theta_v \sin\Theta_s \cos\phi)$, where Θ_v and Θ_s are the view and solar zenith angles and ϕ is the relative azimuth angle, then reject fire pixel if:

$$\Theta_g < 2^\circ$$

or

$$\Theta_g < 10^\circ \text{ and } \rho_5 > 0.1 \text{ and } \rho_7 > 0.2 \text{ and } \rho_{11} > 0.12$$

or

$$\Theta_g < 15^\circ \text{ and } (N_{aw} + N_w) > 0$$

- II. Coast:

Define water pixels as $\rho_{11} < 0.05$ and $\rho_7 < 0.15$ and $NDVI < 0$

Reject fire pixels if the number of presumed-unmasked water pixels $N_{uw} > 0$ and unambiguous fire test is false (N_w is the number of water pixels in search)

- box*; and N_{aw} is the number of water pixels within 8 pixels of candidate fire pixel. $NDVI = (\rho_7 - \rho_5) / (\rho_7 + \rho_5)$
- III. Excessive rejection of legitimate background pixels based on the following criteria:
 $F_b > 0.9$ and $N_b > 3$ and $T'_{13B} < 345$ K and
 $\delta T'_{13B} < 3$ and $\rho_7 > 0.15$ and $T_{13} < (T'_{13B} + 6T'_{13B})$
- IV. Forest clearings:
 Test uses ρ_7 and T_{15} statistics – clearings are cooler and brighter:
 $T_{15} > T_{15B} + 3.7 \delta T_{15}$ AND $\rho_{7B} > 0.28$ AND $T_{13} < 325$ K

Detection confidence is calculated via a combination of statistical variables. See Giglio et al. (2003) for details.

FRP retrievals are calculated for all fire pixels produced by the detection tests above. The VIIRS AF algorithm uses the radiance method of Wooster *et al.* [2003, 2005] to derive FRP in MegaWatts using the following equation:

$$FRP = \frac{S_p \cdot \sigma \cdot (L_F - L_B)}{c} \cdot 10^{-6}$$

Where L_F and L_B are the top-of-atmosphere fire pixel and background radiances ($\text{W} \cdot \text{m}^{-2} \cdot \text{sr}^{-1} \cdot \mu\text{m}^{-1}$) on VIIRS channel M13, σ is the Stefan-Boltzmann constant ($5.6704 \times 10^{-8} \text{ W} \cdot \text{m}^{-2} \cdot \text{K}^{-4}$), S_p is the fire pixel area (m^2), and c is a constant ($2.88 \times 10^{-9} \text{ W} \cdot \text{m}^{-2} \cdot \text{sr}^{-1} \cdot \mu\text{m}^{-1} \cdot \text{K}^{-4}$) calculated for channel M13 following Wooster *et al.* [2003]. The background radiance is estimated using neighboring pixel data based on the same sampling window described above.

2.4. Algorithm Output

The VIIRS AF algorithm output is composed of nine separate data sets (Table 2-2). The fire mask output contains an 8-bit integer two-dimensional array with the same number of elements as the input SDR files. Distinct pixel classes are used for land, water, cloud and fire pixels, plus additional classes indicating non-processed pixels (e.g., missing input data) and pixels with undefined classification. The latter describes those cases when background statistics cannot be retrieved preventing proper classification of the pixel. Three distinct fire pixel classes are used to describe the detection confidence interval according to the following categories: low confidence (0-29%), nominal confidence (30-79%) and high confidence (80-100%). Details describing the calculation of the confidence parameter can be found in Section 2.3.2. A two-dimensional array complements the fire mask output providing quality assurance (QA) information for each pixel in the granule. The QA data contain different fields describing the observation conditions pertinent to each pixel

analyzed. The additional data sets output by the VIIRS AF product include individual sparse arrays containing the list of image line/column, longitude/latitude, FRP, detection confidence, and land/water flag for all fire pixels detected.

Table 2-2: VIIRS AF science data sets. Variable n indicates the number of 48-scan blocks found in a single granule ($n=1$ for NDE granule) (see Section 1.1.1).

Data Set Name	Description	Dimension	Range of Values & Classes
Fire Mask	Image classification product	[3200, $n \times 48 \times 16$]	0 not processed (missing input data) 1 not processed (obsolete) 2 not processed (obsolete) 3 water 4 cloud 5 non-fire clear land 6 unknown 7 low-confidence fire 8 nominal-confidence fire 9 high-confidence fire
Algorithm QA	Fire algorithm quality flags	[3200, $n \times 48 \times 16$]	Bit Field 2 land/water state 2 atmospheric correction 1 day/night state 1 potential fire pixel flag 5 background window size parameter 6 detection test states 3 not used 1 adjacent cloud flag 1 adjacent water flag 2 sun glint level 4 rejection test stats 4 not used
FP Line	Fire pixel line	[N] (number of fire pixels)	Min = 0; Max = $(n \times 48 \times 16) - 1$
FP Column	Fire pixel column	[N] (number of fire pixels)	Min = 0; Max = 3199
FP Longitude	Fire pixel longitude	[N] (number of fire pixels)	Min = 0; Max = ± 180 degrees
FP Latitude	Fire pixel latitude	[N] (number of fire pixels)	Min = 0; Max = ± 90 degrees
FP Power	Fire radiative power	[N] (number of fire pixels)	Scene-dependent (in megawatts)
FP Confidence	Fire pixel confidence	[N] (number of fire pixels)	Min = 0; Max = 100 %
FP Land	Land pixel flag	[N] (number of fire pixels)	1 – land, 0 – water
18 FP diagnostic variables	Variables to describe observing and environmental conditions, and results of algorithm tests	[N] (number of fire pixels)	See netCDF4 metadata

2.5. Performance Estimates

2.5.1. Test Data Description

A set of rigorous tests was performed prior to operations. The offline code was tested for different atmospheric conditions and satellite view angles with regard to fire pixels. Proxy and real Suomi NPP VIIRS SDR data were used as inputs. The outputs were compared to other sensor products; results of these tests are described in following sections.

For the NDE operations, the offline unit test was performed first. All the input data for one particular granule (March 1st, 2015, 05:46-05:48 UTC) were used to test the NDE version and compare the output to the NASA Land SIPS version which is using different data stream and different format (HDF4) for the inputs. All the output parameters were found to be identical in the NDE and NASA versions. Then the code was delivered to the NDE development environment (SADIE) and the algorithm was run there with the same input data.

After it was shown that the SADIE unit test output is identical to the offline version, the code was sent for the NDE system test. At this stage, the algorithm was run in a pre-operational environment on near real-time data. The output for one full day (December 6th, 2015), which consists of about 1000 granules was sent back to developers for verification. This one day output was compared to the same day's offline run on the developers' system, as well as to the current operational (IDPS) product. Following satisfactory results of these comparisons, the system test was continued for about a month with real time data to demonstrate robustness of the process. Full description of all NDE AF test data used in unit and system tests is provided in the NDE AF Algorithm Readiness Review Report (NESDIS/STAR, 2015). This is available by contacting the NDE AF Product Area Lead (PAL) at OSPO.

2.5.2. Sensor Effects

The VIIRS data include a unique aggregation scheme designed to constrain individual sample area growth as a function of scan angle in the cross-track direction, while increasing signal-to-noise ratio [Cao *et al.*, 2014; Wolfe *et al.*, 2013]. This unique data feature can have a positive effect on certain applications [e.g., Schueler *et al.*, 2013], thereby improving upon previous sensors. In the case of the VIIRS AF application, however, the data aggregation has a negative effect leading to reduced algorithm response to small sub-pixel fires. This results from the mixing of fire-free and fire-affected pixel radiances during data aggregation, which will significantly reduce the corresponding aggregated brightness temperature on channel M13. This artificial cooling effect may directly impact the classification of unambiguous fires, as well as the contextual classification of other candidate fire-affected pixels due to the reduced temperature contrast with the background. Potential VIIRS AF algorithm omission errors associated with the data aggregation scheme shall be variable, being dependent on overall observation conditions (e.g., scan angle and atmospheric attenuation) and on specific regional fire regimes (i.e., fire temperature and effective area).

Another indirect effect associated with the aggregation scheme applied to VIIRS data involves the mixing of saturated and unsaturated pixels, in particular the single-gain channel data aggregated onboard the spacecraft. Under those conditions, the aggregated radiance and brightness temperature data will be corrupted whereas the companion quality flags will indicate nominal quality data. The frequency of such anomalies cannot be properly assessed due to the impossibility of dissecting native (pre-aggregation) pixel radiances. However, data simulation analyses suggested that a non-negligible percentage of channel M15 aggregated pixels coinciding with large fires may be subject to mixing of saturated and un-saturated radiances (Figure 2-3).

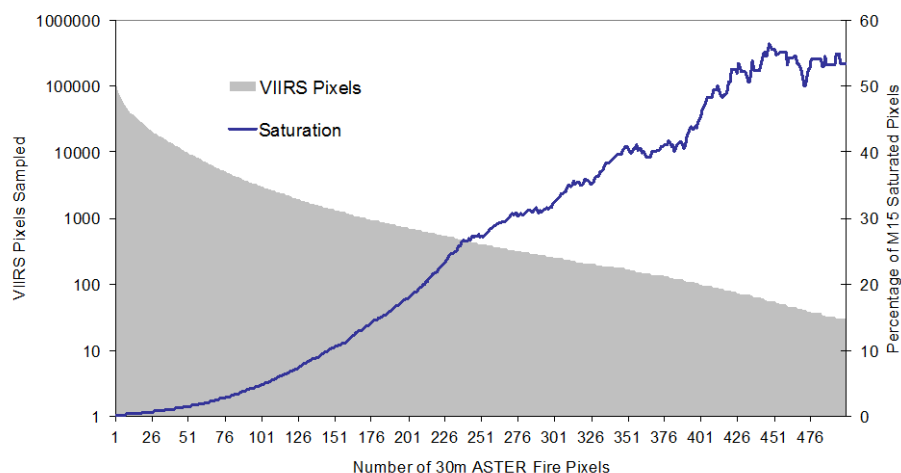


Figure 2-3: Percentage of M15 aggregated pixels resulting from the mixing of saturated and un-saturated native pixels. Results were generated using simulated VIIRS data based on actual Advanced Spaceborne Thermal Emission and Reflection Radiometer (ASTER) 30-m resolution fire-affected pixels.

Compared to other mid-infrared data used for active fire detection (e.g., VIIRS channel I4 and MODIS dual gain channels 21/22), the VIIRS M13 channel spectral response function has a higher wavelength extending into an important CO₂ absorption window. As a result, channel M13 is subject to increased atmospheric attenuation, which could be further magnified when CO₂-rich smoke plumes occupy the sensor's instantaneous field of view. This condition is expected to have a direct effect on the sub-pixel fire characterization retrievals, leading to systematic underestimation of FRP. While numerical simulations using standard atmospheric profiles indicate a potential doubling of the atmospheric attenuation on VIIRS channel M13 compared to VIIRS channel I4 and MODIS channels 21/22 (Figure 2-4), proper quantification of the actual effects associated with smoke plumes on FRP retrievals is currently missing.

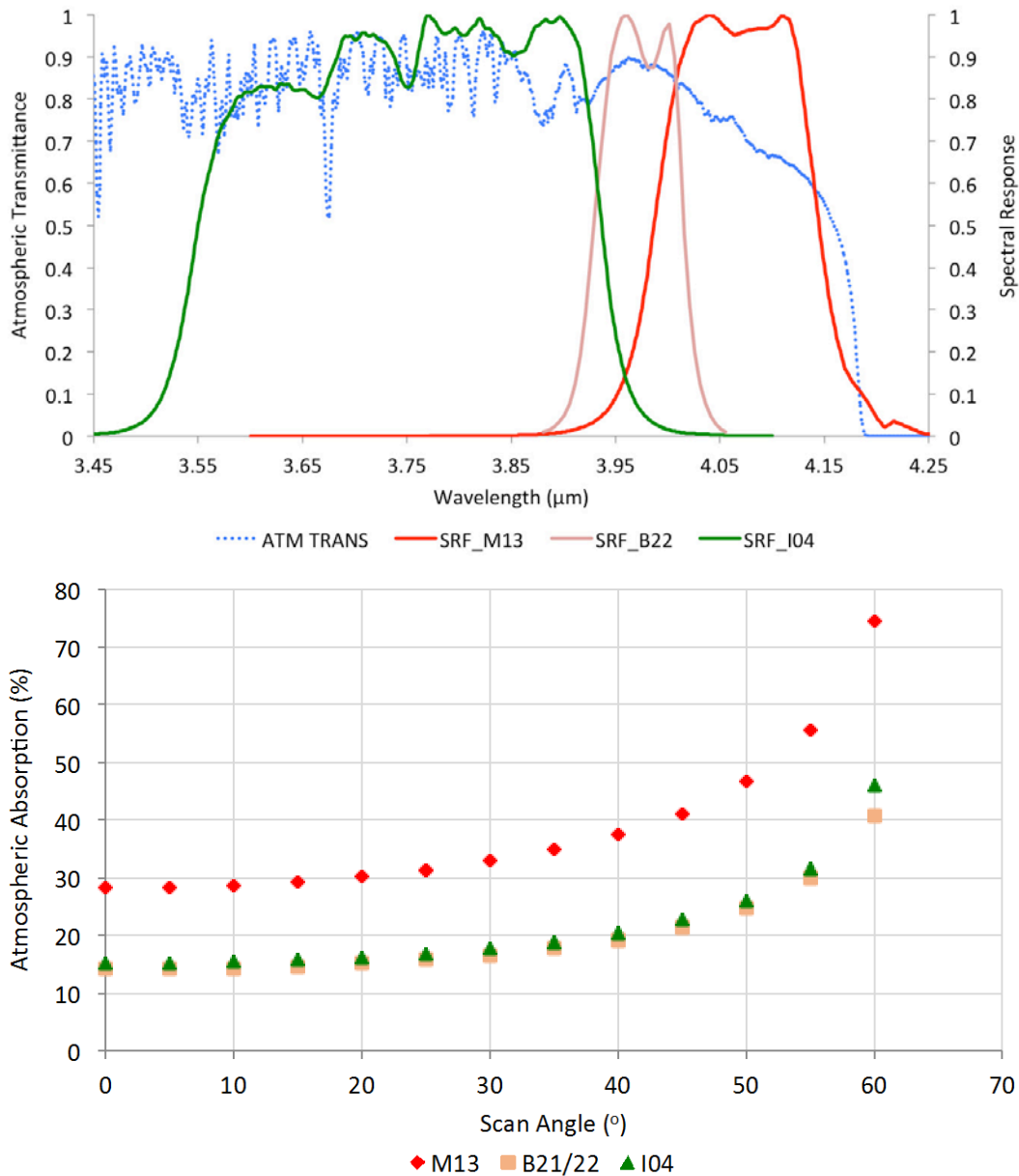


Figure 2-4: Spectral response functions for VIIRS I4 and M13, and MODIS B21/22 mid-infrared channels, and the corresponding atmospheric transmittance calculated using MODTRAN assuming U.S. standard atmospheric conditions (top panel). Bottom panel shows the corresponding net atmospheric absorption as a function of scan angle.

2.5.3. Retrieval Errors

The VIIRS active fire algorithm is a sensor-specific implementation of the heritage MODIS Thermal Anomalies / Fire algorithm. As such the performance of the algorithm can be traced back to MODIS performance, which has been documented via multiple peer-reviewed publications [e.g. Morisette et al., 2005a; Morisette et al., 2005b; Csiszar et al., 2006; Schroeder et al., 2008a; Schroeder et al., 2008b; Csiszar and Schroeder, 2008]. Additionally, some initial evaluations results of the IDPS active fire algorithm are also applicable to the NDE VIIRS AF Product [Csiszar et al., 2014]. Further evaluation is ongoing using independent ground-based and airborne measurements. A major limitation is the high cost of reference data collection and the subsequent lack of statistically robust sample. Explicit validation results are complemented by simulations and correlative analysis with compatible satellite data.

Variable	Estimated error	Data source / methodology
Detection probability	90% probability of detection for a 300m ² fire at 800K ¹	Theoretical simulation
Fire Radiative Power	50%	Correlative analysis with MODIS and DRL TET ²

¹ At nadir, for boreal forest (see Csiszar et al., 2014)

²TET-1: Technology Experiment Carrier-1 by German Aerospace Agency DRL; dedicated 185m unsaturated measurements for hotspot characterization

2.5.4. Numerical Computation Considerations

The Active Fire implementation employs simple tests and does not employ any numerically complex or unstable algorithms.

2.5.5. Programming and Procedural Considerations

There are two processing units in NDE AF: (1) the Preprocessor unit, and (2) the Retrieval unit. Each unit is operated by its own Perl driver script.

The Preprocessor unit performs several important functions.

- It un-packs the input VIIRS SDR data from HDF5 format into binary files. Binary files for VIIRS GEO-Terrain corrected, M13, M15, M16, M5, M7 and M11 are created at

this point.

- It extracts metadata from HDF5 files for subsequent conversion into NetCDF attributes in output NDE AF product. The h5dump utility is used for metadata extraction.
- It creates granulated land-water mask for the granule.

The Retrieval unit performs the following:

- It invokes the AF algorithm which provides all necessary calculations to determine fire locations and properties. It reads SDR input from binary file and provides output fire product as binary file.
- It converts fire output product from binary file into NetCDF format. It reads metadata created at the preprocessor step and converts them into NetCDF attributes.

The Algorithm Development Library (ADL) package is employed at the Preprocessor step for unpacking input data and for land-water mask granulation. The ADL software is a framework that provides similar functionality as the Processing Subsystem in IDPS. It is developed in Raytheon and disseminated as a standalone package. It consists of a number of C++ and Fortran90 subroutines and Perl scripts, as well as a set of commercial off-the-shelf (COTS) libraries included in the package.

At the Retrieval step, the AF source and format conversion codes are employed. They are written in C language.

2.5.6. Quality Assessment and Diagnostics

The VIIRS AF data quality assessment will build on product inter-comparison using near-coincident active fire data from other spaceborne instruments of similar or higher spatial resolution. Preliminary product inter-comparison results using Suomi NPP/VIIRS and Aqua/MODIS near-coincident active fire data showed high level of agreement between the two products (Figure 2-5). Additionally, routine product monitoring will provide summary fire detection metrics and quality flag data for individual scan lines, as well as for global regions at relevant time intervals (e.g., hourly, daily, weekly, monthly).

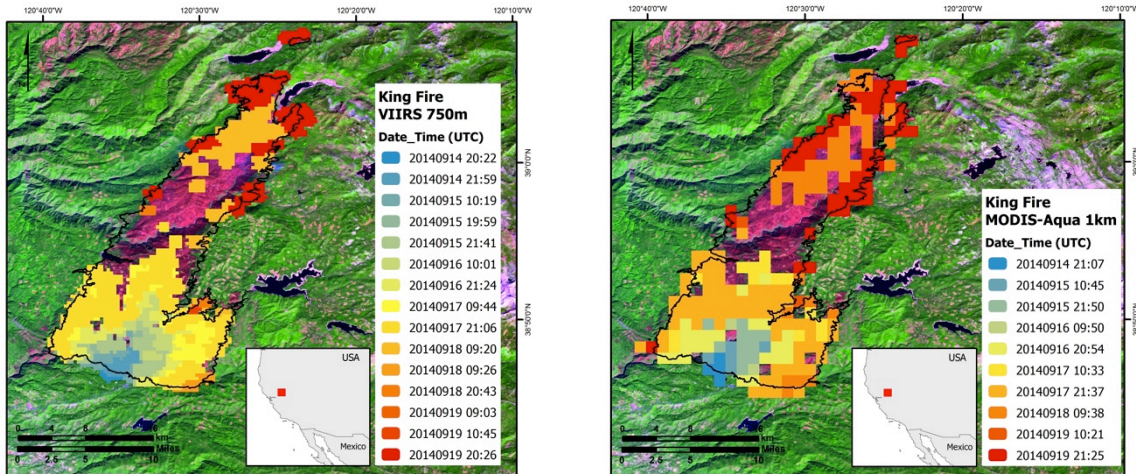


Figure 2-5: S-NPP/VIIRS AF and Aqua/MODIS MYD14 fire detection data produced for the King fire/California on 14-19 September 2014.

2.5.7. Exception Handling

The software checks for bad, missing pixels (denoted by a fill value) and missing input data. It does not perform a retrieval in such cases.

2.6. Validation

VIIRS AF algorithm retrieval errors will be validated using coincident ground-based and high spatial resolution airborne reference data acquired over prescribed fires as well as other fires of opportunity (e.g., wildfires). Currently, availability of quality reference fire data is limited to test-case studies involving ground and airborne sampling of relatively small (<1000 ha) active fires (Figure 2-6).

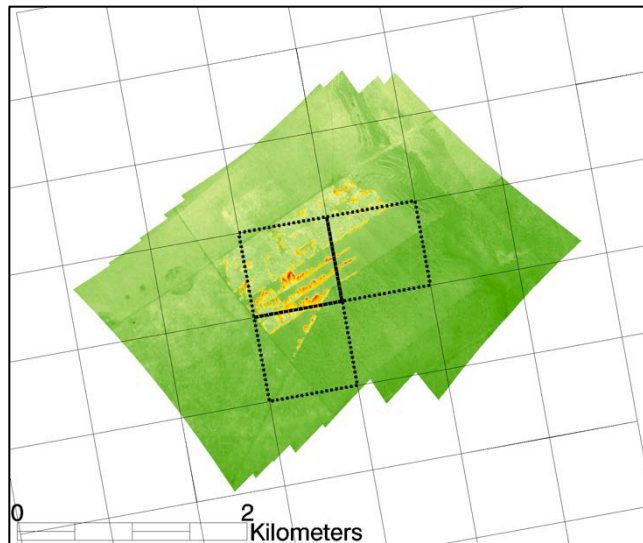


Figure 2-6: Validation of VIIRS AF active fire pixels (marked in thick dashed lines) using airborne reference fire data (background color image, active fires in yellow-red shades) during the Prescribed Fire Combustion and Atmospheric Dynamics Research (RxCADRE) experiment at Eglin Air Force Base/FL, 10 November 2012.

Qualitative reference fire data may be available for larger fire events through USDA Forest Service airborne infrared nighttime data acquisitions. Future validation of VIIRS AF algorithm applied to the JPSS series should support stage 1 validation status, which describes the product's accuracy over a relatively small number of locations.

3. ASSUMPTIONS AND LIMITATIONS

3.1. Performance Assumptions

Algorithm performance is dependent on observation conditions and therefore will be degraded when optically thick clouds and/or heavy smoke plumes are in the line of sight. Typically, higher fire detection omission errors and stronger attenuation of the M13 channel radiance are expected, leading to subsequent underestimation of FRP. Additionally, the pixel's point spread function (PSF) can and will affect product performance, reducing the sensor response to sub-pixel fires and the corresponding probability of detection along with increase in FRP retrieval errors [Schroeder *et al.*, 2010].

3.2. Potential Improvements

Work is ongoing to improve detection performance primarily for nighttime observations. Current results indicate that the criteria for detection are rather conservative. Analysis is being performed to ensure that relaxed detection criteria do not result in the increase of false detections.

4. REFERENCES

List all references to external documents.

- Cao, C., De Luccia, F.J., Xiong, X., Wolfe, R., Weng, F. (2014). Early on-orbit performance of the Visible Infrared Imaging Radiometer Suite onboard the Suomi National Polar-Orbiting Partnership (S-NPP) satellite. *IEEE Transactions on Geoscience and Remote Sensing*, 52, 1142-1156.
- Csiszar, I., Morisette, J., Giglio, L. (2006). Validation of active fire detection from moderate resolution satellite sensors: the MODIS example in Northern Eurasia. *IEEE Transactions on Geoscience and Remote Sensing*, vol. 44, no. 7, 1757-1764.
- Csiszar, I. and W. Schroeder (2008). Short-Term Observations of the Temporal Development of Active Fires from Consecutive Same-Day ETM+ and ASTER Imagery in the Amazon: Implications for Active Fire Product Validation. *IEEE Journal of Selected Topics in Earth Observations and Remote Sensing*, Vol. 1, No. 4, 248-253. DOI: 10.1109/JSTARS.2008.2011377.
- Csiszar, I., Schroeder, W., Giglio, L., Ellicott, E., Vadrevu, K. P., Justice, C. O., Wind, B. (2014). Active fires from the Suomi NPP Visible Infrared Imaging Radiometer Suite: Product status and first evaluation results, *J Geophys Res Atmos*, 119, doi:10.1002/2013JD020453.
- Giglio, L., Descloitres, J., Justice, C. O., Kaufman, Y. J. (2003). An enhanced contextual fire detection algorithm for MODIS. *Remote Sensing of Environment*, 87, 273–282.
- Giglio, L., Schroeder, W., Justice, C.O. (2016). The Collection 6 MODIS Active Fire Detection Algorithm and Fire Products. *Remote Sensing of Environment*, 178 31-41 doi:10.1016/j.rse.2016.02.054.
- Morisette, J.T., Giglio, L., Csiszar, I., Justice, C.O. (2005a). Validation of the MODIS active fire product over Southern Africa with ASTER data. *International Journal of Remote Sensing*, 26:4239–4264.
- Morisette, J.T., Giglio, L., Csiszar, I., Setzer, A., Schroeder, W., Morton, D., Justice, C.O. (2005b). Validation of MODIS active fire detection products derived from two algorithms. *Earth Interactions*, 9:1-23.
- Lobert, J.M., and Warnatz, J. (1993). Emissions from the combustion process in vegetation. In P.J. Crutzen and J.G. Goldammer (Eds.), *Fire in the environment: The ecological, atmospheric, and climatic importance of vegetation fires* (pp. 15-37). John Wiley & Sons Ltd.
- Schroeder, W., Prins, E., Giglio, L., Csiszar, I., Schimdt, C., Morisette, J., Morton, D. (2008a). Validation of GOES and MODIS active fire detection products using ASTER and ETM+ data. *Remote Sensing of Environment*, 112 (2008) 2711–2726.
- Schroeder, W., Ruminiski, M., Csiszar, I., Giglio, L., Prins, E., Schmidt, C., Morisette, J. (2008b): Validation Analyses of and Operational Fire Monitoring Product: the Hazard Mapping System. *International Journal of Remote Sensing*, Vol. 29, No. 20, 6059–6066, DOI: 10.1080/01431160802235845.

- Schroeder, W., Csiszar, I., Giglio, L., and Schmidt, C.C. (2010). On the use of fire radiative power, area, and temperature estimates to characterize biomass burning via moderate to coarse spatial resolution remote sensing data in the Brazilian Amazon. *Journal of Geophysical Research*, 115, doi:10.1029/2009JD013769.
- Schueler, C.F., Lee, T.F., and Miller, S.D. (2013). VIIRS constant spatial resolution advantages. *International Journal of Remote Sensing*, 34, 5761-5777.
- Wolfe, R.E., Lin, G., Nishihama, M., Tewari, K.P., Tilton, J.C., and Isaacman, A.R. (2013). Suomi NPP VIIRS prelaunch and on-orbit geometric calibration and characterization. *Journal of Geophysical Research: Atmospheres*, 118, doi:10.1002/jgrd.50873.
-

END OF DOCUMENT